

## Theoretical investigations of superlattice band structure in the envelope-function approximation

G. Bastard\*

*IBM Thomas J. Watson Research Center, P. O. Box 218, Yorktown Heights, New York 10598*

(Received 26 October 1981)

We extend our previous investigations on the band structure of superlattices by applying the envelope-function approximation to four distinct problems. We calculate the band structure of HgTe-CdTe superlattices and show that these materials can be either semiconducting or zero-gap semiconductors, i.e., behave exactly like the ternary  $\text{Hg}_{1-x}\text{Cd}_x\text{Te}$  random alloys. We analyze the superlattice dispersion relations in the layer planes (Landau superlattice subbands) and we compare the longitudinal and transverse effective masses of semiconducting InAs-GaSb superlattices. We calculate the general equation for the bound states due to aperiodic layers, taking account of the band structure of the host materials. We finally derive the dispersion relations of polytype (*ABC* or *ABCD*) superlattices.

### I. INTRODUCTION

Increasing attention is now paid to the man-made one-dimensional periodic structures, referred to as semiconductor superlattices after Esaki and Tsu.<sup>1</sup> The currently studied GaAs-Ga(Al,As) (Refs. 2 and 3) and InAs-GaSb (Refs. 4 and 5) superlattices are fabricated by molecular beam epitaxy. This technique makes it possible to produce abrupt interfaces between host materials; the interfaces extending only through few lattice planes. Besides their promising technical applications, the superlattices (SL) raise by themselves interesting theoretical problems. Their band structure has been calculated within the linear combination of atomic orbitals (LCAO) framework.<sup>6</sup> A simple computational method, i.e., plane-wave matching,<sup>7</sup> which amounts to be a one-band approximation, worked apparently well in the GaAs-GaAlAs system but completely failed to describe the behavior of InAs-GaSb superlattices.<sup>8</sup> In a recent paper,<sup>9</sup> we have shown that both GaAs-GaAlAs and InAs-GaSb superlattices can be described by the envelope-function (i.e., plane-wave) approximation (EFA) provided that the symmetries of the relevant band edges are correctly taken into account. In the existing SL, one deals with host materials with *S*-type conduction- and *P*-type valence-band edges. Hence, the Kane model<sup>10</sup> is most helpful in describing the electron propagation inside the host layers since it automatically incorporates both conduction- and valence-band edges. Using the Kane-type solutions, we derived the boundary con-

ditions fulfilled by the envelope function at the interfaces. The very simple dispersion relations of the InAs-GaSb SL were found to be in quantitative agreement with the LCAO predictions. This points out the advantages of Kane's model for band-structure calculations using measured parameters such as the effective masses at extrema points.

In contrast with three-dimensional LCAO calculations, very modest computational effort are needed in the EFA. Hence, the EFA is capable of dealing with the SL of arbitrary periods and is applicable to any binary (*A-B*) superlattice, provided that the host's band structures can be described by the Kane model. Within this model, we will end up with two separate descriptions for heavy-hole SL states on the one hand and for coupled light particles (electrons and light holes) SL states on the other hand, provided that  $\vec{k}_\perp$  the carrier wave vector in the layer plane, is equal to zero. If this wave vector is nonzero light and heavy particles will be coupled and we will be able to discuss the SL cyclotron mass. The flexibility and generality of the EFA have inspired us to extend our previous analysis to several problems connected with SL band structure. The EFA will be discussed in Sec. II and applied to the case of HgTe-CdTe superlattices (Sec. III). The dispersion relations and SL effective masses (i.e., longitudinal or transverse with respect to the SL growing axis) will be discussed in Sec. IV. Section V will be devoted to interface defect states which arise from an irregular layer thickness. Finally, in Sec. VI, we will apply the EFA method to *ABC* or *ABCD*-type superlattices.

## II. THE ENVELOPE-FUNCTION APPROXIMATION

Consider two semiconductors  $A$  and  $B$ . The  $AB$  superlattice consists of alternating layers of  $A$  and  $B$  materials. In what follows, we shall take the  $z$  axis to be parallel to the SL axis. Longitudinal and transverse will, respectively, mean "along the SL axis" or perpendicular to this axis (i.e., in the layer plane). Inside each host material the electron states are assumed to be describable by the Kane model. The valence ( $P$ -like) and conduction ( $S$ -like) edges are at the center of the Brillouin zone.

$$\mathcal{H} = \begin{pmatrix} |S, M_J = -\frac{1}{2}\rangle & |S, M_J = +\frac{1}{2}\rangle & |P, M_J = +\frac{3}{2}\rangle & |P, M_J = +\frac{1}{2}\rangle & |P, M_J = -\frac{1}{2}\rangle & |P, M_J = -\frac{3}{2}\rangle \\ 0 & 0 & 0 & 0 & \Pi_{c,v} \sqrt{2/3} \hbar k_A & 0 \\ 0 & 0 & 0 & \Pi_{c,v} \sqrt{2/3} \hbar k_A & 0 & 0 \\ 0 & 0 & -\epsilon_A & 0 & 0 & 0 \\ 0 & \Pi_{c,v} \sqrt{2/3} \hbar k_A & 0 & -\epsilon_A & 0 & 0 \\ \Pi_{c,v} \sqrt{2/3} \hbar k_A & 0 & 0 & 0 & -\epsilon_A & 0 \\ 0 & 0 & 0 & 0 & 0 & -\epsilon_A \end{pmatrix}, \quad (1)$$

where

$$\Pi_{c,v} = \frac{-i}{m_0} \langle S | P_x | X \rangle.$$

The free-electron kinetic energy has been neglected. This is consistent with our neglect of the remote band effects. The dispersion relations are

$$\epsilon = -\frac{\epsilon_A}{2} + \frac{\epsilon_A}{2} \left[ 1 + \frac{8\Pi_{c,v}^2}{3\epsilon_A^2} \hbar^2 (k_A)^2 \right]^{1/2}. \quad (2)$$

Each eigensolution of (1) is doubly degenerate with respect to the  $z$  projection of the total angular momentum. The values  $M_J = \pm \frac{1}{2}$  correspond to light particles (electrons and light holes). They are completely decoupled from the  $M_J = \pm \frac{3}{2}$  states which, as may be seen from Eq. (1), have no component on the  $|S, M_J = \pm \frac{1}{2}\rangle$  states and are in fact dispersionless. The  $M_J = \pm \frac{3}{2}$  states correspond to the heavy-hole solutions. A finite heavy-hole mass can be restored only if one accounts for  $\vec{k} \cdot \vec{p}$  interaction between the  $|P, M_J = \pm \frac{3}{2}\rangle$  states and the remote bands of the crystal (see below). The decoupling between  $|S, M_J = \pm \frac{1}{2}\rangle$  and  $|P, M_J = \pm \frac{3}{2}\rangle$  states holds only if  $\vec{k}_\perp = \vec{0}$ . It arises from the fact that both  $\vec{J}$  and  $\vec{k}$  have been taken to be parallel to the SL axis. For homogeneous  $A$

The spin-orbit coupling lifts the sixfold valence degeneracy at  $k=0$  into a  $\Gamma_8$  quadruplet and a  $\Gamma_7$  doublet. For our purpose, the  $\Gamma_7$  doublet can be neglected. Since the spin-orbit coupling is quite large, the  $\vec{k} \cdot \vec{p}$  interaction is exactly diagonalized with the  $\Gamma_6, \Gamma_8$  basis. The electronic motion inside each layer ( $A$  or  $B$ ) is described by  $k_A$  or  $k_B$  and  $\vec{k}_\perp = (k_x, k_y)$ . Note that the transverse wave vector  $\vec{k}_\perp$  is conserved across an interface since in the EFA the interface potential depends only on  $z$ . If  $\vec{k}_\perp = \vec{0}$ , the Kane matrix describing the  $\vec{k} \cdot \vec{p}$  interaction within the  $\Gamma_6, \Gamma_8$  subspace is particularly simple. For instance, in  $A$  material it reads

or  $B$  materials, the choice of the quantization axis is somewhat arbitrary (if one neglects nonspherical terms like  $\Gamma_8$  warping or inversion asymmetry splitting). In superlattices, on the other hand, the  $z$  axis is, in practice, chosen along the SL axis; this choice making the interface equations analytically trivial. If, however, the  $z$  direction is fixed and  $\vec{k}_\perp \neq \vec{0}$ , the coupling between  $M_J = \pm \frac{3}{2}$  and  $M_J = \pm \frac{1}{2}$  states is nonzero. The origin of this coupling may be traced back to the fact that the most general spherically symmetric, quadratic  $\Gamma_8$   $\mathcal{H}$  is not the scalar  $C_2 k^2$ , but rather

$$\mathcal{H} = C_1 k^2 + C_2 (\vec{k} \cdot \vec{J})^2. \quad (3)$$

We have emphasized this point since it significantly influences the results of Sec. IV.

In  $B$  layers, at  $\vec{k}_\perp = \vec{0}$ , the effective  $\mathcal{H}$  is obtained by shifting the  $\Gamma_6(S)$  origin by  $V_S$  and the  $\Gamma_8$ -band edges by  $V_P$ . In principle one should also change  $\Pi_{c,v}^{(A)}$  into  $\Pi_{c,v}^{(B)}$ . However, the Kane matrix element  $\Pi_{c,v}$  does not change very much from one III-V compound to another, which in fact witnesses the similarities between the periodic part of the Bloch functions in various III-V semiconductors. Therefore, we will assume that  $\Pi_{c,v}^{(A)}$  is the same as  $\Pi_{c,v}^{(B)}$ . This will avoid introduction of extra  $[\Pi_{c,v}(z), d/dz]$  in the foregoing analysis [e.g., in

Eq. (7)].

If we are interested in the slowly varying envelope functions and discard any phenomena rapidly varying on the scale of host unit cells, these envelope functions are the solutions of a  $6 \times 6$  differential system obtained from  $\mathcal{H}$  [Eq. (1)] by changing  $\hbar k_z$  into  $-i\hbar d/dz$  and by letting the  $S$  and  $P$  edges be position dependent through the relations

$$V_{S,P}(z+md) = V_{S,P}(z), \quad (4)$$

$$V_{S,P}(z) = 0 \quad \text{if } 0 \leq z \leq l_A, \quad (5)$$

$$V_{S,P}(z) = V_{S,P} \quad \text{if } l_A \leq z \leq l_A + l_B,$$

where  $l_A$  and  $l_B$  are the  $A$ - and  $B$ -layer thickness, respectively, and  $d = l_A + l_B$  is the SL period. On the scale of variations of the envelope functions, the interfaces reduce to the planes

$$\begin{aligned} z &= l_A + md, \\ z &= pd, \end{aligned} \quad (6)$$

where  $m$  and  $p$  are integers. Since we neglect any variations occurring on the scale of host unit cells, the SL medium is translationally invariant in the layer planes, and  $\vec{k}_\perp$  is a good quantum number. Owing to the fact that we neglect  $\vec{k} \cdot \vec{p}$  coupling between  $\Gamma_8$  states and the remote bands of the hosts, the  $6 \times 6$  differential system can be easily transformed into a  $2 \times 2$  differential system, nonlinear in  $\epsilon$ , which governs the envelope functions associated with the  $|S, M_J = +\frac{1}{2}\rangle$  and  $|S, M_J = -\frac{1}{2}\rangle$  states. If  $\vec{k}_\perp = \vec{0}$  a further simplification occurs. Rearranging Eq. (1) one transforms the  $6 \times 6$  problem into two identical  $1 \times 1$  equations decoupled from two identical and independent  $2 \times 2$  differential systems describing the coupled behavior of envelope functions associated with  $|S, M_J = +\frac{1}{2}\rangle$  and  $|P, M_J = +\frac{1}{2}\rangle$  and with  $|S, M_J = -\frac{1}{2}\rangle$  and  $|P, M_J = -\frac{1}{2}\rangle$ , respectively. These identical  $2 \times 2$  systems are

$$\begin{bmatrix} V_S(z) - \epsilon & \Pi_{c,v} \sqrt{2/3} P_z \\ \Pi_{c,v} \sqrt{2/3} P_z & -\epsilon_A + V_P(z) - \epsilon \end{bmatrix} \begin{bmatrix} F_S(z) \\ F_P(z) \end{bmatrix} = 0, \quad (7)$$

where  $F_S$  and  $F_P$  are the slowly varying envelope functions associated with  $|S\rangle$  and  $|P\rangle$  states, respectively, and  $P_z = -i\hbar(d/dz)$ . Projecting onto the  $S$  state one further transforms the system [Eq. (7)] into a differential equation which is nonlinear in  $\epsilon$

$$\begin{aligned} & \left[ 2 \frac{\Pi_{c,v}^2}{3} P_z [\epsilon_A + \epsilon - V_P(z)]^{-1} P_z + V_S(z) \right] F_S(z) \\ & = \epsilon F_S(z). \end{aligned} \quad (8)$$

To complete the problem, we impose on  $F_S(z)$  the Bloch condition

$$F_S(z+md) = \exp(iqmd) F_S(z), \quad (9)$$

where  $q$  is the SL wave vector along the SL direction and  $m$  is an integer. At the  $A$ - $B$  interface, we integrate Eq. (8) across the boundary and, if  $F_S$  is assumed to be continuous, we obtain

$$\begin{aligned} & [\epsilon_A + \epsilon - V_P(z)]^{-1} \frac{dF_S}{dz}(z), \\ & \text{continuous at the interface.} \end{aligned} \quad (10)$$

This equation, already derived in Ref. 9, has also been recently obtained by White and Sham.<sup>11</sup> It generalizes Ben Daniel and Duke's result,<sup>12</sup>

$$\frac{1}{m^*(z)} \frac{dF}{dz}, \quad \text{continuous at the interface,}$$

to the case of nonparabolic materials, i.e., to materials in which the band mixing is important. It is therefore of crucial use in the type-II superlattices (InAs-GaSb) in which one has to admix predominantly  $S$ -type electrons with predominantly  $P$ -type light holes to build the superlattice states.

Inside  $A$  and  $B$  layers,  $V_S$  and  $V_P$  are constant and the eigenstates of Eq. (8) are a linear combination of two plane waves with opposite wave vectors. There are, therefore, four unknown coefficients to be determined by four equations. The wave functions  $F_S(z)$  are nonvanishing only if

$$\begin{aligned} \cos qd &= \cos k_A l_A \cos k_B l_B \\ & - \frac{1}{2} (\xi + \xi^{-1}) \sin k_A l_A \sin k_B l_B, \end{aligned} \quad (11)$$

$$\xi = \frac{k_A}{k_B} \frac{\epsilon_A + \epsilon - V_P}{\epsilon_A + \epsilon}. \quad (12)$$

This dispersion relation (11) is, of course, the same if one projects the system equation (7) on the  $P$  state rather than on the  $S$  state.

If the energy  $\epsilon$  does not correspond to a propagating state in  $A$  or  $B$  layer,  $k_A$  or  $k_B$  is imaginary (evanescent states). Finally, no SL exists if both  $k_A$  and  $k_B$  are imaginary owing to the Bloch equation (9). Note that Eqs. (11) and (12) are quite general, describing the band structure of any  $A$ - $B$  superlattice provided that the relevant host electronic states are well described by the Kane model.

A. Heavy-hole dispersion relations at  $\vec{k}_\perp = \vec{0}$ —  
effect of effective-mass gradients

As for the heavy-hole dispersion relations, they are identically  $\epsilon=0$  or  $\epsilon=V_p$ , corresponding to SL heavy-hole states which are entirely localized within *A* or *B* layers. More embarrassing is the lack of one-dimensional quantization originating from the absence of finite heavy-hole masses. These shortcomings are cured by introducing the quadratic effective  $\mathcal{H}$  for heavy holes. If (and only if)  $\vec{k}_\perp = \vec{0}$ , the  $\Gamma_8$   $\mathcal{H}$  [Eq. (3)] is diagonal in the  $|P, M_J\rangle$  basis, and for  $m_J = \pm \frac{3}{2}$ , one has simply

$$\begin{aligned} \langle P, \pm \frac{3}{2} | \mathcal{H} | P, \pm \frac{3}{2} \rangle &= (-\gamma_1^{(A)} + 2\gamma^{(A)}) P_z^2 \\ &= -\frac{P_z^2}{2M_A} \quad \text{if } 0 \leq z \leq l_A. \end{aligned} \quad (13)$$

In Eq. (13) the  $\gamma_1$  and  $\gamma$  are the Luttinger parameters describing the  $\vec{k} \cdot \vec{p}$  interaction between the  $|P \pm \frac{3}{2}\rangle$  states and the remote bands of the hosts. Along the same line one should also add to the system (7) a term  $(\gamma_1 + 2\gamma)P_z^2$  in the  $F_p$  diagonal term. This term is small and does not bring any new qualitative insight to the previous analysis. We will henceforth neglect it. As for the  $|P \pm \frac{3}{2}\rangle$  states, let us stress the fact that the effective masses  $M_A$  and  $M_B$  are in general different; one must solve the differential equation

$$\left\{ \frac{1}{4} [P_z^2, M_{hh}^{-1}(z)] + V_p(z) \right\} F_{hh}(z) = \epsilon F_{hh}(z), \quad (14)$$

where  $\{A, B\} = AB + BA$ ;  $V_p(z)$  is defined in Eqs. (4) and (5) and

$$\begin{aligned} M_{hh}(z) &= M_A, \quad 0 \leq z \leq l_A \\ M_{hh}(z) &= M_B, \quad l_A \leq z \leq l_A + l_B \\ M_{hh}(z + md) &= M_{hh}(z) \end{aligned} \quad (15)$$

for any relative integer  $m$ . In contrast to the usual Kronig-Penney situation, we see that both valence-band edges and effective masses are position dependent. Even if there is no valence-band offset ( $V_p=0$  for any  $z$ ) band gaps will still exist in the heavy-hole SI band structure due to the periodic variation of the heavy-hole effective mass.

To complete Eq. (14), boundary conditions should be added. Again, we impose the Bloch condition Eq. (9) on  $F_{hh}$ . Integrating Eq. (14) across an interface, assuming  $F_{hh}(z)$  to be continuous and using the fact that  $M_{hh}(z)$  is piecewise constant, the boundary condition becomes

$$M_{hh}^{-1}(z) \frac{dF_{hh}(z)}{dz} \quad (16)$$

continuous at the interface. Consider the probability density  $\rho_{hh}(z) = |F_{hh}(z)|^2$ ; it fulfills the continuity equation

$$\frac{\partial \rho_{hh}}{\partial t} + \frac{\partial J_{hh}}{\partial z} = 0 \quad (17)$$

with

$$J_{hh}(z) = -\frac{i\hbar}{2M_{hh}(z)} \left[ F_{hh}^*(z) \frac{d}{dz} F_{hh}(z) - \text{cc} \right]. \quad (18)$$

For a stationary state one has simply

$$J_{hh}(z) = \text{const.} \quad (19)$$

Therefore, if at the *A-B* interface  $F_{hh}(z)$  is assumed continuous, the  $M_{hh}^{-1}(z)dF_{hh}/dz$  continuity and *not* the  $dF_{hh}/dz$  continuity will ensure the constancy of  $J_{hh}$ , i.e., the time independence of the  $\rho_{hh}$ .<sup>12</sup>

Building the SL wave function inside the unit cell ( $0 \leq z \leq d$ ) in the same way as before, we finally obtain the SL heavy-hole dispersion relations,

$$\begin{aligned} \cos qd &= \cos k_A l_A \cos k_B l_B \\ &\quad - \frac{1}{2}(\eta + \eta^{-1}) \sin k_A l_A \sin k_B l_B, \end{aligned} \quad (20)$$

where

$$\eta = \frac{k_A M_B}{k_B M_A}. \quad (21)$$

Note that Eq. (20) is similar in form to the light-particles dispersion relation (11). In fact, this form is quite general and is obtained for any *A-B* superlattice problem, even if the band edges  $V_S(z)$  and  $V_p(z)$  were position dependent inside each host layer.<sup>13</sup> The details of  $V_p(z)$ ,  $V_S(z)$ , and of the boundary conditions are embedded in the energy dependence of the parameter  $\eta$ .

### III. BAND STRUCTURE OF HgTe-CdTe SUPERLATTICES

The HgTe-CdTe superlattices have not yet been fabricated. They are, however, conceptually quite interesting because, in contrast to GaAs-GaAlAs or InAs-GaSb superlattices, the relevant host electronic states belong to  $\Gamma_8$  bands. Schulman and McGill<sup>14</sup> have numerically calculated their band structure within the three-dimensional LCAO framework. They were, therefore, limited to rather small SL periods and, for this reason, do not reach general conclusions concerning the trend of the

HgTe-CdTe SL band structure. The EFA is again capable of providing a complete and simple description. CdTe is a standard wide-gap semiconductor ( $\epsilon_B \sim 1.6$  eV), whereas HgTe is a symmetry-induced zero-gap semiconductor. In HgTe, both conduction and valence bands have  $\Gamma_8$  ( $P, J = \frac{3}{2}$ ) symmetry at the center of the Brillouin zone. The  $\Gamma_6$  ( $S, J = \frac{1}{2}$ ) levels lie below the  $\Gamma_8$  edges. Hence, the interaction gap  $\epsilon_A = \epsilon_{\Gamma_6} - \epsilon_{\Gamma_8}$  is negative, whereas in standard (e.g. CdTe) materials  $\epsilon_B = \epsilon_{\Gamma_6} - \epsilon_{\Gamma_8}$  is positive (Fig. 1).

One does not know the valence-band offset between HgTe and CdTe. The common anion argument and the similarity of the host's lattice constants have led Schulman and McGill to assume it to be zero. We shall use here the same assumption. Both host material's band structures are of the Kane type and we may use the results obtained in Sec. II.

At  $\vec{k}_\perp = \vec{0}$  the heavy-hole  $|P, M_J = \pm \frac{3}{2}\rangle$  levels are completely decoupled from the light-particle levels that arise from  $\vec{k} \cdot \vec{p}$  hybridization of  $|P, M_J = \pm \frac{1}{2}\rangle$  with  $|S, M_J = \pm \frac{1}{2}\rangle$ . Since the relevant band edges are  $\Gamma_8$  levels, we choose the energy zero at the top of the heavy-hole valence band and we project the  $2 \times 2$  system equation (7) onto the  $P$  level. The  $F_P(z)$  envelope functions are, therefore, the eigenstates of

$$\frac{2}{3} \Pi_{c,v}^2 P_z [\epsilon - V_S(z) - \epsilon_A]^{-1} P_z F_P(z) + V_P(z) F_P(z) = \epsilon F_P(z), \quad (22)$$

where  $\epsilon_A < 0$  is the negative HgTe interaction gap and  $V_P(z) = 0$  since there is no valence-band offset. The boundary conditions are therefore

$$F_P(z), \quad [\epsilon - V_S(z) - \epsilon_A]^{-1} \frac{dF_P(z)}{dz}, \quad \text{continuous at the interface} \quad (23)$$

and

$$F_P(z + md) = \exp(iqmd) F_P(z).$$

The SL dispersion relations are given by Eq. (11) with

$$\xi = \frac{k_A}{k_B} \frac{\epsilon - \epsilon_B}{\epsilon + |\epsilon_A|}. \quad (24)$$

The methodological interest of HgTe-CdTe SL lies in the fact that the light particles of host materials have effective masses of opposite signs but the same band-edge symmetry. In fact, if one neglects

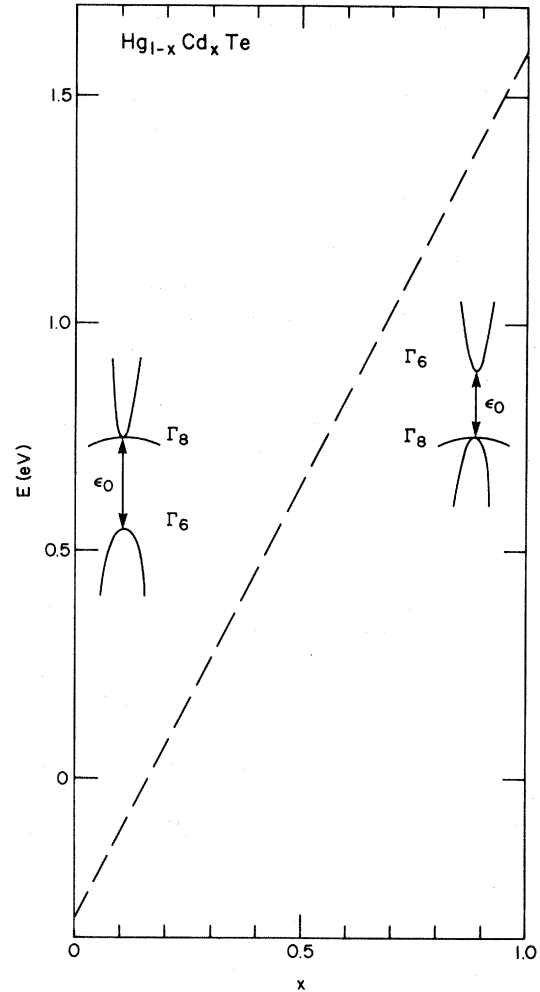


FIG. 1. Band structure of  $\text{Hg}_{1-x}\text{Cd}_x\text{Te}$  random alloys vs the composition  $x$  (virtual-crystal approximation). The dashed line represents the variation of  $\epsilon_0$  with  $x$ .

the band nonparabolicity, viz, neglects  $\epsilon$  with respect to  $|\epsilon_A|$ ,  $\epsilon_B$  one gets

$$\xi = \frac{k_A}{k_B} \frac{m_B}{m_A}, \quad m_B < 0.$$

This formula is the same as that for conduction superlattice states in GaAs-GaAlAs superlattices where the host's band edges are  $S$ -like<sup>9</sup> or for heavy-hole SL dispersion relations [see Eq. (21)].

For  $\epsilon > 0$ ,  $k_B$  is imaginary, whereas if  $\epsilon < 0$ ,  $k_A$  is imaginary. It is interesting to observe that  $\epsilon = 0$  is an allowed state in the SL. It corresponds to  $q = 0$ . Hence,  $\epsilon = 0$  is either the top of the highest light-hole subband  $LH_1$  or the bottom of the lowest electron subband  $E_1$ , or both. An expansion of the dispersion relation in the vicinity of  $\epsilon = 0$

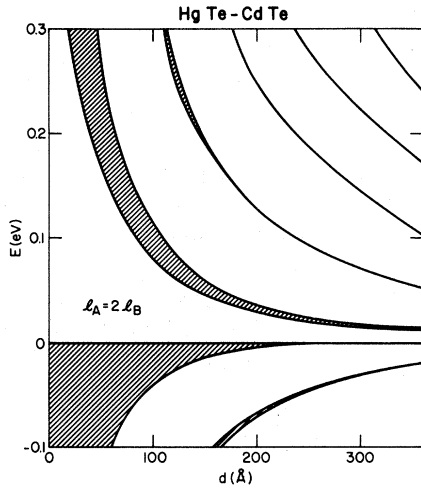


FIG. 2. Evolution of the band structure of HgTe-CdTe SL's vs the SL period  $d$ . Only the light particles bands are shown.  $l_A/l_B=2$ ,  $k_1=0$ . The allowed energy bands are shaded.

( $\epsilon > 0$ ) shows the lack of allowed SL states if

$$\frac{l_A}{l_B} < \frac{\epsilon_B}{|\epsilon_A|} \sim 5.3. \quad (25)$$

Conversely, for Hg-rich SL ( $l_A/l_B > \epsilon_B/|\epsilon_A|$ ), the first conduction subband  $E_1$  starts at  $\epsilon=0$  and the  $LH_1$  top is located at some finite negative energy. For the critical  $l_A/l_B$  ratio ( $\epsilon_B/|\epsilon_A|$ ),  $LH_1$  and  $E_1$  touch at  $q=0$ . Moreover, the dispersion relations are linear in  $q$  ( $q \rightarrow 0$ ) for this peculiar composition. As for the heavy-hole subbands, they are readily obtained from Eqs. (17) and (18). Since the

valence-band offset is assumed to be zero, the energy  $\epsilon=0$  is always a SL solution corresponding to  $q=0$ : The last heavy-hole subband  $HH_1$  ends at  $\epsilon=0$ . Collecting all these information we see the following.

(1) If  $l_A/l_B < \epsilon_B/|\epsilon_A|$ , the HgTe-CdTe SL are semiconducting. The SL fundamental gap is equal to  $E_1(q=0) - HH_1(q=0)$ .

(2) If  $l_A/l_B > \epsilon_B/|\epsilon_A|$ , the HgTe-CdTe SL are zero-gap semiconductors with the  $E_1$  and  $HH_1$  subbands touching at  $q=0$ .

(3) If  $l_A/l_B = \epsilon_B/|\epsilon_A|$ , the HgTe-CdTe SL are zero-gap semiconductors with a heavy-hole band quadratic in  $q$  and two light bands linear in  $q$ .

The HgTe-CdTe superlattices behave then exactly in the same way as do the ternary random alloys  $\text{Hg}_{1-x}\text{Cd}_x\text{Te}$ .<sup>15</sup> In the virtual-crystal approximation, these solid solutions display the HgTe zero-gap structure if  $x < 0.16$ , i.e., if the  $[\text{Hg}]/[\text{Cd}]$  ratio  $> 0.84/0.16 = \epsilon_B/\epsilon_A$ . If on the other hand,  $x > 0.16$ , the  $\text{Hg}_{1-x}\text{Cd}_x\text{Te}$  solid solutions are narrow-gap semiconductors with the CdTe band structure (see Fig. 1). At this zero-gap-to-semiconductor transition ( $x=0.16$ ) there is a triple band degeneracy and the heavy-hole band is quadratic in  $k$ , whereas the electron- and light-hole bands are linear in  $k$ .

Finally, owing to the imaginary  $k_A$  or  $k_B$  one should expect narrow SL bands. We illustrate this point in Fig. 2, which shows the evolution of the HgTe-CdTe SL band structure (for light particles only) with increasing periodicity  $d$  when  $l_A=2l_B$ .

#### IV. TRANSVERSE DISPERSION RELATIONS—COMPARISON BETWEEN LONGITUDINAL AND TRANSVERSE EFFECTIVE MASSES

When  $\vec{k}_1 \neq \vec{0}$ , the procedure we applied in Sec. II [Eqs. (1)–(7)] is still of relevance. Projecting onto the  $S$  states leads to  $2 \times 2$  differential system:

$$\begin{bmatrix} \mathcal{H}_{11}(\epsilon) & \mathcal{H}_{12}(\epsilon) \\ \mathcal{H}_{21}(\epsilon) & \mathcal{H}_{22}(\epsilon) \end{bmatrix} \begin{bmatrix} F_1 \\ F_2 \end{bmatrix} = \epsilon \begin{bmatrix} F_1 \\ F_2 \end{bmatrix}, \quad (26)$$

where

$$\begin{aligned} \mathcal{H}_{11}(\epsilon) = \mathcal{H}_{22}(\epsilon) = & V_S(z) + \Pi_{c,v}^2 P_- [\epsilon_A + \epsilon - V_P(z)]^{-1} P_+ \\ & + \frac{\Pi_{c,v}^2}{3} P_+ [\epsilon_A + \epsilon - V_P(z)]^{-1} P_- + \frac{2\Pi_{c,v}^2}{3} P_z [\epsilon_A + \epsilon - V_P(z)]^{-1} P_z, \end{aligned} \quad (27)$$

$$\mathcal{H}_{12} = \mathcal{H}_{21}^* = \Pi_{c,v}^2 \sqrt{2}/3 \{ P_z [\epsilon_A + \epsilon - V_P(z)]^{-1} P_+ - P_+ [\epsilon_A + \epsilon - V_P(z)]^{-1} P_z \}, \quad (28)$$

where

$$P_{\pm} = (P_x \pm iP_y) / \sqrt{2}. \quad (29)$$

The 1 and 2 indices play the part of spin  $\downarrow$  and spin  $\uparrow$  quantum states in a band structure which is otherwise characterized by a strong spin-orbit coupling.  $\mathcal{H}_{12}$  then reflects the mixing of  $|\uparrow\rangle$  and  $|\downarrow\rangle$  states induced by the combined action of the scalar  $\vec{k} \cdot \vec{p}$  and interface  $V_S(z)$ ,  $V_P(z)$  potentials with the host's spin-orbit coupling. That  $\mathcal{H}_{12}$  exactly vanishes if the spin-orbit coupling  $\Delta_{so}$  vanishes is immediately seen if one uses the natural basis  $S\uparrow, S\downarrow; X\uparrow, \downarrow; Y\uparrow, \downarrow; Z\uparrow, \downarrow$  for  $\Delta_{so}=0$ . If using the  $\Gamma_6, \Gamma_7, \Gamma_8$  basis, well suited to nonzero  $\Delta_{so}$ , one should first reintroduce the  $\Gamma_7$  states and then let  $\Delta_{so}$  vanish. The existence of  $\mathcal{H}_{12}$  analogs is well known in narrow-gap semiconductor physics.<sup>16-18</sup>

In magneto-optics, the combined action of  $\Delta_{so}$  and radiation electric fields allows for the existence of electric dipole spin-flip resonance if  $k \neq 0$ .<sup>16</sup> The finite  $\Delta_{so}$  and the band nonparabolicity are responsible for anomalous Hall effect observed, e.g., in InSb.<sup>17</sup> In narrow-gap metal-oxide–semiconductor (MOS) structures, Ohkawa and Uemura<sup>18</sup> have already discussed the combined effect of  $\Delta_{so}$ ,  $\vec{k} \cdot \vec{p}$  interaction and the surface electric field. They predicted anomalously large surface electron  $g$  factors.

The coupling term  $\mathcal{H}_{12}$  increases with  $\vec{k}_1$ . Its explicit  $k_1$  dependence implies that the SL dispersion relations  $\epsilon(q, k_1)$  cannot be simply obtained by using appropriate  $k_A(\vec{k}_1)$  and  $k_B(\vec{k}_1)$  in Eqs. (11) and (12). Instead, explicit and tedious calculations are required.

Before giving the results of these calculations, we need to discuss the  $\vec{k}_1$ -induced coupling between heavy-hole and light-particle states. In Sec. II, we showed that the light particles decouple from heavy holes if  $\vec{k}_1 = \vec{0}$ . We were then justified in discarding remote-band effects on the light-particle dispersion relations and in calculating  $E_n(k_1=0)$  and  $LH_n(k_1=0)$  with  $M_{hh} = \infty$ . Subsequently, we obtained  $HH_n$  by introducing the heavy-hole curvature. At  $\vec{k}_1 = \vec{0}$  the remote-band effects exactly reduce to the (diagonal) heavy-hole kinetic energy. At  $\vec{k}_1 \neq \vec{0}$  this agreeable simplification no longer holds. The explicit  $6 \times 6$  matrix which reduces to Eq. (1) at  $\vec{k}_1 = \vec{0}$  now contains a whole nonzero  $(4 \times 4)$   $\Gamma_8$  block. Its explicit form is known.<sup>19</sup> Still, it displays several terms involving  $k_1 P_z$  which spoils any simplification like a simple projection on the  $|S\uparrow\rangle$  and  $|S\downarrow\rangle$  band-

edge states. We have not been able to overcome these difficulties and to treat the problem  $\vec{k}_1$  different from  $\vec{0}$  exactly. We have then followed the same decoupling procedure as at  $\vec{k}_1 = \vec{0}$ :

(1) For light-particles dispersion relations, we have neglected the remote-band effects, which amounts to dealing with a diagonal  $\Gamma_8$  block in the general  $6 \times 6$  matrix.

(2) For heavy-hole states, the  $\Gamma_8$  block is treated in the parabolic approximation. The remote and the  $\Gamma_6$  band are taken into account up to the order  $k^2$ . This procedure amounts to changing the  $\gamma_1$  and  $\gamma$  parameters into  $\tilde{\gamma}_1$  and  $\tilde{\gamma}$  with

$$\begin{aligned} \tilde{\gamma}_1 \begin{bmatrix} A \\ B \end{bmatrix} &= \gamma_1 \begin{bmatrix} A \\ B \end{bmatrix} + 2m_0 \Pi_{c,v}^2 / 3\epsilon_B^A, \\ \tilde{\gamma} \begin{bmatrix} A \\ B \end{bmatrix} &= \gamma \begin{bmatrix} A \\ B \end{bmatrix} + m_0 \Pi_{c,v}^2 / 3\epsilon_B^A. \end{aligned} \quad (30)$$

This decoupling procedure is expected to be good for all SL states if, at  $\vec{k}_1 = \vec{0}$ , the  $E_n$  and  $HH_n$  states are energetically well separated. This is, for instance, the case in GaAs-GaAlAs or in semiconducting InAs-GaSb superlattices. The semimetallic InAs-GaSb superlattices are a notable exception. In these materials,  $E_1(k_1=0)$  is very close to or degenerate with  $HH_1(k_1=0)$  and  $HH_2(k_1=0)$ . Suppose, for instance, that at  $k_1=0$ ,  $E_1(q=0, k_1=0) < HH_1(q=0, k_1=0)$ . Tuning  $k_1$  (experimentally the magnetic field) would cause  $E_1(q=0, k_1)$  to cross  $HH_1(q=0, k_1)$ , since  $E_1$  is predominantly InAs electronlike and  $HH_1$  GaSb heavy-hole-like. This crossing takes place at  $k_1 \neq 0$ ; it is likely that  $E_1$  will in fact not cross  $HH_1$ . A correct description of this anticrossing requires an exact calculation of the  $k_1$  dependence of all SL states, which is beyond the scope of our decoupling scheme. Keeping these reservations in mind, we have calculated the light-particle dispersion relations neglecting remote-band effects. The  $2 \times 2$  system (26)–(29) is completed by the boundary conditions:

$$\begin{aligned} F_1(z), \quad [\epsilon_A + \epsilon - V_P(z)]^{-1} \left[ -\sqrt{2} \frac{dF_1}{dz} - ik_+ F_2 \right], \\ F_2(z), \quad [\epsilon_A + \epsilon - V_P(z)]^{-1} \left[ -\sqrt{2} \frac{dF_2}{dz} + ik_- F_1 \right], \end{aligned} \quad (31)$$

all continuous at the  $A - B$  interface, and

$$F_{1,2}(z) \exp(iqmd) = F_{1,2}(z + md). \quad (32)$$

The boundary conditions provide us with eight homogeneous equations in eight unknowns (two plane-wave amplitudes per layer and per "spin"). Setting the determinant of this  $8 \times 8$  system to zero leads to two identical dispersion relations. These are

$$\begin{aligned} \cos qd &= \cos k_A l_A \cos k_B l_B \\ &- \frac{1}{2} \left[ \xi + \xi^{-1} + \frac{k_1^2}{4k_A k_B} (r + r^{-1} - 2) \right] \\ &\times \sin k_A l_A \sin k_B l_B, \end{aligned} \quad (33)$$

where

$$\xi = \frac{k_A}{k_B} r, \quad r = \frac{\epsilon_A + \epsilon - V_P}{\epsilon_A + \epsilon}, \quad (34)$$

$$\frac{2}{3} \Pi_{c,v}^2 \hbar^2 (k_A^2 + k_1^2) = \epsilon(\epsilon + \epsilon_A), \quad (35)$$

$$\frac{2}{3} \Pi_{c,v}^2 \hbar^2 (k_B^2 + k_1^2) = (\epsilon - V_S)(\epsilon + \epsilon_A - V_P). \quad (36)$$

The twofold degeneracy is expected since there is no external magnetic field. Note also that  $\vec{k}_1$  enters the dispersion relations only through  $k_1^2$ ; this accounts for the cylindrical symmetry around the SL axis. Finally, let us remark that the whole SL band structure and especially the SL bandwidths are  $k_1$  dependent. In other words, SL bands are not only  $k_1$  shifted but also deformed with  $k_1$ . Apart from the explicit  $k_1$  dependence of Eq. (33), which is entirely due to the nonvanishing  $\mathcal{H}_{12}$ , the  $\epsilon(q)$  dispersion relations are obtained as if host band structures were different for different  $k_1$ . For instance, in the InAs-GaSb system, one deals with an effective  $k_1$ -dependent overlap between the InAs conduction band and the GaSb light-hole level; this overlap decreases with increasing  $k_1$  (Fig. 3). It is then natural that the  $E_1$  bandwidth decreases with increasing  $k_1$  corresponding to SL states, which are more localized at finite  $k_1$  than at  $k_1 = 0$ . For very large  $k_1$ , the  $E_1$  bandwidth may even become negligible. We illustrate this point in Fig. 4 where we show the evolution of  $\Gamma_1$ , the  $E_1$  bandwidth, versus  $k_1^2$  for two InAs-GaSb superlattices with (30–50)-Å and (65–80)-Å layer thicknesses, respectively.

The most convenient techniques to study SL dispersion relations are the Shubnikov–de Haas effects and the far-infrared magnetoabsorption. If

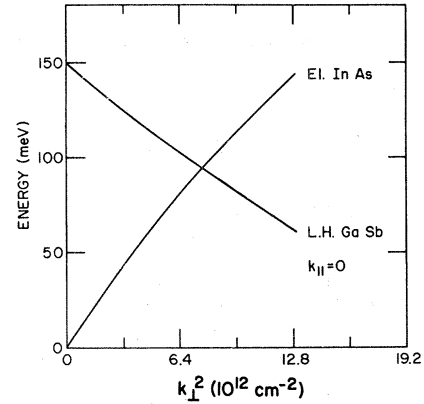


FIG. 3. GaSb (light-hole) and InAs (conduction-) band-edge energies are plotted vs  $k_1^2$  to illustrate the decrease of the effective overlap between the light-particle state from which the SL states are built. The component  $k_{\parallel}$  of the wave vector parallel to the SL axis is set equal to zero.

one neglects the spin effects, our  $k_1$  calculation can be translated into Landau-level patterns by using the quantization rule

$$k_1^2 = (2n + 1)/\lambda^2, \quad (37)$$

where  $\lambda = (\hbar c / eH)^{1/2}$  is the usual magnetic length. Figure 5 shows the calculated Landau levels belonging to the lowest electronic subband  $E_1$  at  $q = 0$  for semiconducting InAs-GaSb superlattices. We have also shown in this figure the semiempirical dispersion relations

$$\begin{aligned} \epsilon \left( 1 + \frac{\epsilon}{\epsilon_A} \right) &= E_1(q=0, k_1=0) \\ &\times \left[ 1 + \frac{E_1(q=0, k_1=0)}{\epsilon_A} \right] \\ &+ \left( n + \frac{1}{2} \right) \frac{\hbar e H}{m_A c} \end{aligned} \quad (38)$$

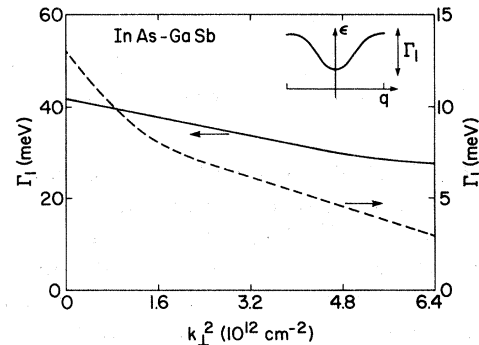


FIG. 4.  $E_1$  bandwidth  $\Gamma_1$  is plotted vs  $k_1^2$  for two InAs-GaSb SL's:  $l_A, l_B = 30$  and  $50$  Å (left scale) and  $65$  and  $80$  Å (right scale).

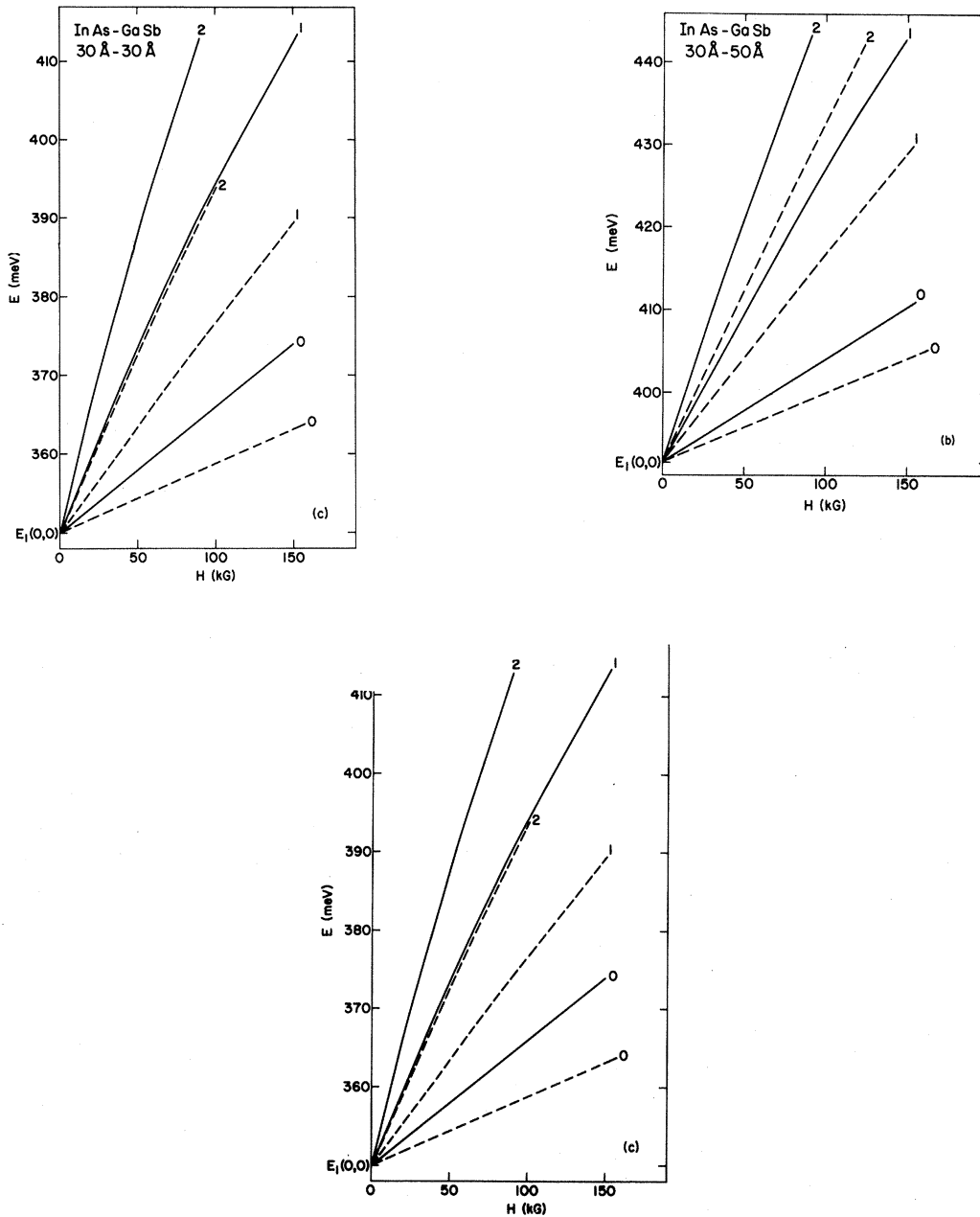


FIG. 5. Calculated Landau-level patterns at  $q=0$  for three different InAs-GaSb SL's. (a)  $l_A, l_B=65$  and  $80$  Å; (b)  $30$  and  $50$  Å; (c)  $30$  and  $30$  Å. The dashed lines represent the semiempirical result (38).

( $A \equiv \text{InAs}$ ), which has proved successful in interpreting several oscillatory phenomena in the InAs-GaSb system.<sup>20-22</sup> Equation (38) is based on the assumption that  $E_1(q=0, k_1)$  SL states are mostly built from InAs conduction states, for which a Kane-type treatment is appropriate. For the (65–80)-Å sample, both models almost agree if  $n \neq 0$ . In this sample, far-infrared magneto-optical experiments<sup>20</sup> have shown a broad cyclotron line

corresponding to  $1 \rightarrow 2$  or  $3 \rightarrow 4$  cyclotron resonances depending on the laser frequency. Both Eq. (38) and our model give an acceptable agreement between calculations and experiments. The Landau-level patterns are, however, sensitively different if  $E_1(q=0, k_1=0)$  increases (short-periods SL) or thick GaSb layers. When expressed in terms of a transverse mass  $m_1$ , our calculations lead to much lighter  $m_1$  than Eq. (38) in InAs-

GaSb superlattices with large  $E_1(q=0, k_\perp=0)$ . That the two models should differ is clear from the lack of any explicit  $d, l_A, l_B$  dependences in Eq. (38). Hence, in this model two SL with different  $d, l_A, l_B$  but the same  $E_1(q=0, k_\perp=0)$  should have the same Landau levels. These Landau levels are, in principle, different according to our calculations. The difference between the two models ultimately arises from the InAs confinement assumption underlying the semiempirical approach. This assumption works well in large periodicity SL [as witnessed by the good agreement between Eq. (38) and the far-infrared data obtained in the semimetallic InAs-GaSb SL (Refs. 21 and 22)]. We believe it should fail if  $\Gamma_1(k_\perp)$  is noticeable, i.e., if the electron appreciably penetrates in GaSb layers. Experiments are needed to elucidate this point.

Quite generally, we may define the SL band-edge effective masses  $m_\perp$  and  $m_\parallel$ : For  $E_1$ , we define

$$E_1(q, k_\perp) = E_1(0, 0) + \frac{\hbar^2 q^2}{2m_\parallel} + \frac{\hbar^2 k_\perp^2}{2m_\perp}. \quad (39)$$

The masses  $m_\parallel$  and  $m_\perp$  can be analytically obtained from Eq. (33). The resulting expressions are, however, cumbersome and of little use. It is more instructive to relate  $m_\parallel$  and  $m_\perp$  to the  $qp_z$  and  $\vec{k}_\perp \cdot \vec{p}$  perturbation expansion on the exact  $q=0, k_\perp=0$  superlattice states. In doing so, we eliminate the  $k_\perp$ -induced light-heavy particle coupling and may safely describe whole InAs-GaSb family. We have

$$\frac{1}{m_\perp} = \frac{1}{m_0} + \frac{2}{m_0^2} \sum_{X_n} \frac{|\langle E_1, 0, 0 | P_x | X_n, 0, 0 \rangle|^2}{E_1(0, 0) - X_n(0, 0)}, \quad (40)$$

$$\frac{1}{m_\parallel} = \frac{1}{m_0} + \frac{2}{m_0^2} \sum_{X_n} \frac{|\langle E_1, 0, 0 | P_z | X_n, 0, 0 \rangle|^2}{E_1(0, 0) - X_n(0, 0)}.$$

in Eq. (40) the summation over  $X_n$  includes all but  $E_1$  SL states (light-particle and heavy-hole states) at the center of the SL Brillouin zone. There exist two  $|E_1, 0, 0\rangle$  states corresponding to a given  $M_J$ . Each of these states is  $P_z$  connected with all the  $|E_n, 0, 0\rangle$  and  $|LH_n, 0, 0\rangle$  states of the same  $M_J$ . The operator  $P_z$  has, however, no nonvanishing element between  $|E_1, 0, 0\rangle$  and  $|HH_n, 0, 0\rangle$ . On the other hand,  $P_x$  connects the  $|E_1, 0, 0\rangle$  level with  $M_J = \pm \frac{1}{2}$  to the  $|HH_n, 0, 0\rangle$  states of  $M_J = \pm \frac{3}{2}$  but also with the  $|E_n, 0, 0\rangle$  and  $|LH_n, 0, 0\rangle$  levels corresponding to  $M_J = \pm \frac{1}{2}$ .

The lack of  $qp_z$  interaction between  $E_1$  and  $HH_n$  and

$$\langle E_1, 0, 0 | P_x | HH_n, 0, 0 \rangle \neq 0$$

have some interesting consequences on the behavior of  $m_\parallel$  and  $m_\perp$  with SL periodicity in the InAs-GaSb system. In this system, there exists a semiconductor  $\rightarrow$  semimetal (SC $\rightarrow$ SM) transition resulting from the inversion of the relative positions of  $E_1(0, 0)$  and  $HH_1(0, 0)$ . For equal InAs and GaSb thicknesses, this SC $\rightarrow$ SM transition takes place near  $d \sim 185 \text{ \AA}$ .<sup>4,5,9</sup> At this transition nothing particular occurs to the longitudinal mass  $m_\parallel$  since  $E_1$  and  $HH_1$  are not  $P_z$  coupled. Such is not the case for  $m_\perp$ . Since

$$\langle E_1, 0, 0 | P_x | HH_1, 0, 0 \rangle \neq 0,$$

one expects the  $k_x P_x$  coupling between  $E_1$  and  $HH_1$  to dominate the remaining terms in Eq. (40). Therefore,  $m_\perp$  should vanish at the SC $\rightarrow$ SM transition and change sign from SC to SM sides. Note that this sign reversal is currently met in II-VI mixed crystals like the  $\text{Hg}_{1-x}\text{Cd}_x\text{Te}$  alloys: At critical composition  $x \simeq 0.16$  the  $\Gamma_6$  band passes through the  $\Gamma_8$  edges and its masses changes sign. Note also that such a mass reversal is absent from the semiempirical approach of Eq. (38).

It is, however, very likely that the  $m_\perp$  sign reversal will take place in a very narrow  $d$  range. The reason is the smallness of the coupling matrix element  $\langle E_1, 0, 0 | P_x | HH_1, 0, 0 \rangle$  because of the important spatial confinement of  $E_1$  into InAs and  $HH_1$  into GaSb layers, respectively. To dominate the remaining terms in Eq. (40), the  $P_x$  coupling between  $E_1$  and  $H_1$  should take place between extremely close  $E_1$  and  $H_1$  states [ $E_1(0, 0) - HH_1(0, 0)$  being in the meV range]. This is in contrast to II-VI alloys where the  $\Gamma_6$ - $\Gamma_8$  coupling is predominant for  $\epsilon_{\Gamma_6} - \epsilon_{\Gamma_8}$  gaps as large as 0.3 eV. Symmetrically,  $HH_1$  will exhibit a  $m_\perp$  sign reversal at the SC $\rightarrow$ SM transition but again this anomaly will not be easy to detect. For equal InAs and GaSb thicknesses,  $E_1(0, 0)$  becomes very close to  $LH_1(0, 0)$  for  $d \simeq 230 \text{ \AA}$  ( $E_1$  and  $LH_1$  actually anticross). Hence, a very light  $m_\parallel$  mass can be expected for  $E_1$ . Again the two-band ( $E_1$  and  $LH_1$ ) situation will prevail only near  $d \simeq 230 \text{ \AA}$  since, as before, the involved  $P_z$  matrix element will be rather small owing to the pronounced localization of  $E_1$  and  $LH_1$  states into different layers.

We have numerically calculated  $m_\parallel$  and  $m_\perp$  according to Eq. (33) in the InAs-GaSb system for equal layer thicknesses. Owing to our oversimplified decoupling procedure  $m_\perp$  cannot be reliably obtained above the SC $\rightarrow$ SM transition, whereas  $m_\parallel$  can be calculated for arbitrary  $d$ . The results

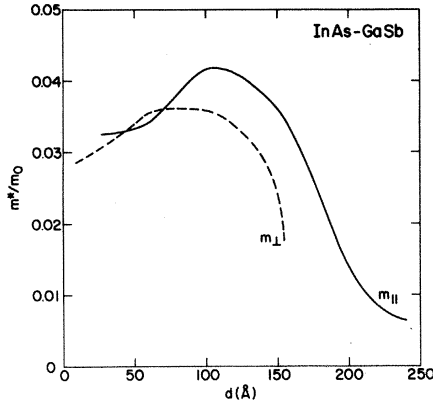


FIG. 6. Evolution of the  $E_1$  transverse ( $m_{\perp}$ ) and longitudinal ( $m_{\parallel}$ ) SL effective masses with the period  $d$  for InAs-GaSb SL's of equal-layer thicknesses.

are shown on Fig. 6. One sees that  $m_{\parallel}$  and  $m_{\perp}$  are quite light in small-period superlattices. Moreover, the mass anisotropy is not very large ( $\leq 20\%$ ) at small  $d$ . The longitudinal effective mass  $m_{\parallel}$  decreases with  $d$ , approaching  $6 \times 10^{-3} m_0$  near the  $E_1$ - $LH_1$  anticrossing. Plotting  $m_{\parallel}$  vs  $E_1(0,0) - LH_1(0,0)$  gives us a rough estimate of the  $\langle E_1, 0, 0 | P_z | LH_1, 0, 0 \rangle$  matrix element in the vicinity of the anticrossing. We have obtained

$$\frac{2}{m_0} |\langle E_1, 0, 0 | P_z | LH_1, 0, 0 \rangle|^2 \simeq 0.9, \quad (41)$$

in units of eV, which has to be compared with the Kane matrix element

$$\frac{2}{m_0} |\langle S | P_z | Z \rangle|^2 \sim 19,$$

in units of eV, found in usual III-V and II-VI semiconductors.

## V. INTERFACE DEFECT STATES

Consider a  $A$ - $B$  superlattice with period  $d = l_A + l_B$ , and assume that one of the  $A$  layers is irregular with a thickness  $L_A$ . We choose the  $z$  origin at the left side of the irregular  $A$  layer. We want to calculate the wave function and the energy position of the  $A$ -type bound state associated with this defect. If  $L_A > l_A$ , we know that at least one such bound state exists since we are dealing with a one-dimensional problem. The very same problem was recently treated by Combescot and Benoit à la Guillaume<sup>23</sup> in the simple plane-wave approach assuming moreover equal valence and conduction

masses. Restricting themselves to the infinitely deep quantum wells, Voisin *et al.*<sup>24</sup> have recently studied the bound states created by trenchlike defects. Here we want to show that the EFA allows a complete and simple treatment of the planar interface defects, taking exactly into account the host material band structures. We, therefore, adopt all the notations used in Sec. II.

If there exists a bound state at the energy  $\epsilon$ , its wave function decreases exponentially when  $z \rightarrow \pm \infty$ . The Bloch condition (9) should then be replaced by

$$F_S(z + md) = \exp(-qmd) F_S(z), \quad (42)$$

$$F_S(-z - md) \exp(-qmd) F_S(-z),$$

$$z \geq 0, \quad m > 0.$$

Let us assume for simplicity  $\vec{k}_{\perp} = \vec{0}$ . The boundary conditions at the  $A$ - $B$  interfaces are the same as before [Eq. (10)]. Writing these boundary conditions when going from the  $N$ th unit cell to the  $(N + l$ th) [ $L_A + l_B + Nd \leq z \leq L_A + l_B + (N + 1)d$ ] and making use of Eq. (42), one obtains the "dispersion relations"

$$\cosh(qd) = \cos k_A l_A \cos k_B l_B - \frac{1}{2}(\xi + \xi^{-1}) \sin k_A l_A \sin k_B l_B, \quad (43)$$

where all the symbols have the same meaning as in Sec. II. We also obtain the ratio of incoming and outgoing plane waves in the  $B$  layer. Hence, in the irregular unit cell ( $0 < z < L_A + l_B$ ) the wave function for  $L_A < z < L_A + l_B$  is entirely known (apart from a normalization coefficient). Writing the continuity equations at  $z = L_A$  provides us with two equations linking the two unknown coefficients ( $C_1$  and  $C_2$ ) in the anomalous  $A$  layer to the two coefficients in the neighboring  $B$  layer. Finally, one eliminates the  $B$ -layer coefficients and gets one homogeneous equation linking the two unknowns  $C_1$  and  $C_2$ . The same procedure is repeated for negative  $z$ . The dispersion relation (43) is again obtained as well as the ratio of the two plane-wave amplitudes inside the  $B$  layer. In the final step, one writes the boundary conditions at  $z = 0$  and reduces the problem to two homogeneous linear equations for the two unknown coefficients  $C_1$  and  $C_2$ . The energy position of the bound level is then determined by solving

$$\begin{aligned} \exp(qd) [\cos k_B l_B \cos k_A L_A \\ - \frac{1}{2}(\xi + \xi^{-1}) \sin k_B l_B \sin k_A L_A] \\ = \cos k_A l_A \cos k_A L_A + \sin k_A l_A \sin k_A L_A, \quad (44) \end{aligned}$$

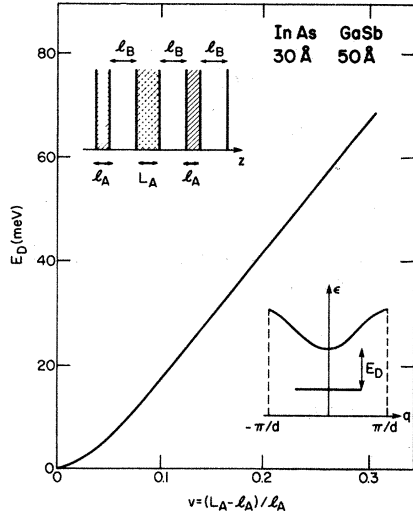


FIG. 7. Binding energy  $E_D$  of the ground interface defect bound state plotted vs  $v = (L_A - l_A) / l_A$  the relative thickness of the anomalous InAs layer in a 30-Å–50-Å InAs-GaSb SL.

where  $qd$  is obtained from Eq. (43). The bound-state equation is again quite general and may be applied to any kind of binary SL. To illustrate the previous results, we have calculated the bound state created by an anomalous InAs layer in the InAs-GaSb SL system. Luminescence experiments were performed on a (30–50) Å InAs-GaSb SL. For this SL, the lowest-lying ( $E_1$ ) conduction band extends from 392 to 433 meV (the energy zero being taken at the bulk InAs conduction-band edge). In Fig. 7, we show the binding energy  $E_D$  of the InAs defect versus  $v = (L_A - l_A) / l_A$ , which is the relative excess thickness of the InAs anomalous layer. One sees that the binding energy is quite substantial (41 meV) for  $v = 0.2$ . The value  $v = 0.2$  roughly corresponds to an extra InAs thickness of two InAs atomic planes. If  $v$  is large enough, a second

$$F_S(z) = \alpha_A \exp(ik_A z) + \beta_A \exp(-ik_A z), \quad 0 \leq z \leq l_A$$

$$F_S(z) = \alpha_B \exp[ik_B(z - l_A)] + \beta_B \exp[-ik_B(z - l_A)], \quad l_A \leq z \leq l_A + l_B \quad (45)$$

$$F_S(z) = \alpha_C \exp[ik_C(z - l_A - l_B)] + \beta_C \exp[-ik_C(z - l_A - l_B)], \quad l_A + l_B \leq z \leq l_A + l_B + l_C.$$

We can write the boundary conditions (10) for  $F_S$  and its derivative at the  $A$ - $B$  and  $B$ - $C$  interfaces. This gives us

$$\begin{bmatrix} \alpha_B \\ \beta_B \end{bmatrix} = T_{A \rightarrow B} \begin{bmatrix} \alpha_A \\ \beta_A \end{bmatrix}, \quad \begin{bmatrix} \alpha_C \\ \beta_C \end{bmatrix} = T_{B \rightarrow C} \begin{bmatrix} \alpha_B \\ \beta_B \end{bmatrix}, \quad (46)$$

and the Bloch theorem reads

( $v \sim 1.5$ ), third, etc., bound state appears. Ultimately, when  $v \rightarrow \infty$  one should recover the InAs impurity modes  $k_A L_A = p\pi, p = 1, 2$ .

Since the transverse motion is free in regular and anomalous layer, a steplike density of states is associated to each of the  $A$ -type bound states. In real SL, many irregular  $A$  slices of different  $v$  exist. Hence, several  $A$ -type bound states together with  $B$ -type bound levels will be found in the forbidden gap. The identification of these defect states will be quite difficult. The difficulty is further increased by the fact that trenchlike<sup>24</sup> or shoeboxlike irregularities may also give rise to bound impurity states. Note also that the shallow impurities do not produce well-defined hydrogenic impurity states but are smeared out into impurity bands due to the dependence of the binding energy on the impurity position.<sup>25</sup>

## VI. POLYTYPE SUPERLATTICES BAND STRUCTURE

Our calculations have been so far restricted to binary ( $A$ - $B$ ) superlattices. It may prove useful for specific technological purposes to grow ternary ( $A$ - $B$ - $C$ ), quaternary ( $A$ - $B$ - $C$ - $D$ ), etc., SL. Esaki, Chang, and Mendez<sup>26</sup> recently proposed this novel idea and applied it to the case of InAs-GaSb-AlSb multiheterojunctions. The calculations of  $A$ - $B$ - $C$ -type SL band structure will be almost unfeasible in the three-dimensional LCAO framework unless  $l_A, l_B, l_C$  are only a few atomic planes thick. On the other hand, the EFA is capable of achieving this task. To do so, let us use the transfer matrix scheme. Consider a given  $ABC$  superlattice unit cell and assume for simplicity  $\vec{k}_1 = \vec{0}$ . Inside each layer the projection  $F_S(z)$  of the wave function on the  $S$  level is a sum of incoming and outgoing plane waves:

$$\begin{bmatrix} \alpha_A \\ \beta_A \end{bmatrix} \exp(iqd) = T_{C \rightarrow A} \begin{bmatrix} \alpha_C \\ \beta_C \end{bmatrix}. \quad (47)$$

( $\alpha_A, \beta_A$ ) is then the eigenvector corresponding to the eigenvalue  $e^{iqd}$  of the transfer matrix

$$\tau = T_{C \rightarrow A} T_{B \rightarrow C} T_{A \rightarrow B}. \quad (48)$$

To find the eigenvalue of  $\tau$   $\det\tau$  has to be 1 and the solutions are such that<sup>6</sup>

$$2\cos(qd) = \text{Tr}(\tau). \quad (49)$$

Let us choose the energy zero at the bottom of the *S*-type band of the *A* material. Define  $V_P^{B,A}$  and  $V_P^{C,A}$  the energy shifts of the *P* edges between *A* and *B*, *A*, and *C* materials, respectively. In terms of the quantities

$$\begin{aligned} \xi_{A,B} &= \frac{k_A}{k_B} \frac{\epsilon_A + \epsilon - V_P^{A,B}}{\epsilon_A + \epsilon}, \\ \xi_{B,C} &= \frac{k_B}{k_C} \frac{\epsilon_A + \epsilon - V_P^{C,A}}{\epsilon_A + \epsilon - V_P^{B,A}}, \\ \xi_{C,A} &= \frac{k_C}{k_A} \frac{\epsilon_A + \epsilon}{\epsilon_A + \epsilon - V_P^{C,A}}, \end{aligned} \quad (50)$$

which are such the  $\xi_{A,B}\xi_{B,C}\xi_{C,A} = 1$ , the dispersion relations obtained from Eq. (49) are

$$\begin{aligned} \cos(qd) &= \cos k_A l_A \cos k_B l_B \cos k_C l_C \\ &\quad - \frac{1}{2}(\Omega_{B,C} \cos k_A l_A \sin k_B l_B \sin k_C l_C + \Omega_{C,A} \sin k_A l_A \cos k_B l_B \sin k_C l_C \\ &\quad + \Omega_{A,B} \sin k_A l_A \sin k_B l_B \cos k_C l_C) \end{aligned} \quad (51)$$

with

$$\Omega_{X,Y} = \xi_{X,Y} + \xi_{X,Y}^{-1}, \quad (52)$$

where  $q$  is the SL wave vector and  $d = l_A + l_B + l_C$ , the SL period. This procedure can be clearly iterated. For instance, the dispersion relations of *ABCD*-type SL are obtained in terms of  $\xi_{A,B}, \xi_{B,C}, \xi_{C,D}, \xi_{D,A}$ :

$$\begin{aligned} \cos(qd) &= \cos k_A l_A [\cos k_B l_B \cos k_C l_C \cos k_D l_D - \frac{1}{2}(\xi_{C,D} \xi_{B,C} + \xi_{C,D}^{-1} \xi_{B,C}^{-1}) \sin k_B l_B \cos k_C l_C \sin k_D l_D \\ &\quad - \frac{1}{2} \Omega_{C,D} \sin k_C l_C \sin k_D l_D \cos k_B l_B - \frac{1}{2} \Omega_{B,C} \sin k_B l_B \sin k_C l_C \cos k_D l_D] \\ &\quad - \frac{1}{2} \sin k_A l_A [(\xi_{A,B} \xi_{B,C} + \xi_{A,B}^{-1} \xi_{B,C}^{-1}) \cos k_D l_D \cos k_B l_B \sin k_C l_C \\ &\quad - (\xi_{B,C} \xi_{D,A} + \xi_{B,C}^{-1} \xi_{D,A}^{-1}) \sin k_B l_B \sin k_C l_C \sin k_D l_D \\ &\quad + \cos k_C l_C (\Omega_{A,B} \sin k_B l_B \cos k_D l_D + \Omega_{D,A} \sin k_D l_D \cos k_B l_B)], \end{aligned} \quad (53)$$

where all the symbols have the same meaning as before except that  $d$  is now equal to  $l_A + l_B + l_C + l_D$ .

Let us remark that for the *A,B,C* system there exist in principle two possible ternary SL's built from these elements. There are the *A,B,C* and *A,C,B* materials. However, the sequence *ACBCB*... is *ABCABC*... spelled backward. Therefore, the SL potentials  $V_{ACB}(z)$  and  $V_{ABC}(z)$  are such that  $V_{ACB}(z) = V_{ABC}(-z)$ . The Bloch eigenstates  $\psi_{ABC}(z)$  and  $\psi_{ACB}(z)$  of the same energy correspond to SL states of opposite wave vector  $q$  and  $-q$ . But  $\epsilon(q) = \epsilon(-q)$  and the dispersion relations of *ABC* and *ACB* SL's are, therefore, identical. This is in fact apparent in Eq. (51) which is invariant under any permutation of *A*, *B*, and *C*. For quaternary SL such a simplification does not occur and the *ABCD*, *ACBD* SL's should have different band structures.

## VIII. CONCLUSION

We have extended our previous work on the EFA to four distinct SL problems. For all these problems, the EFA has enabled us to obtain entirely analytical solutions. We believe that no other computation method (LCAO, etc.) would have achieved this task. We have shown that HgTe-CdTe SL's may display either a finite or a zero-gap semiconductor configuration; the zero-gap  $\rightarrow$  semiconductor transition taking place for a host thickness ratio  $l_{\text{HgTe}}/l_{\text{CdTe}}$  which is exactly the same as the  $[\text{HgTe}]/[\text{CdTe}]$  ratio for which the ternary *random* alloy  $\text{Hg}_{1-x}\text{Cd}_x\text{Te}$  undergoes the same transition. We have derived and discussed the transverse SL dispersion relations of *A-B*-type SL's. We have shown that the transverse SL effective mass  $m_{\perp}$  in the InAs-GaSb system should undergo

a sign reversal when the lowest electric band  $E_1$  crosses the highest heavy-hole band  $HH_1$ . This sign reversal will, however, be very hard to detect due to the small  $p_x$  matrix element between  $E_1$  and  $HH_1$ . We have derived the bound-state equation for planar interface defects in superlattices, taking exactly into account the host band structure. This equation is valid for any kind of  $A$ - $B$  SL. Finally, we have obtained the dispersion relations of polytype superlattices ( $A$ - $B$ - $C$  or  $A$ - $B$ - $C$ - $D$  systems). Owing to a  $\bar{k}_\perp$ -induced light-particle-heavy-hole coupling, our EFA calculations require further elab-

orations and refinements to reliably describe the Landau levels of semimetallic InAs-GaSb SL's.

#### ACKNOWLEDGMENTS

All the calculations and results obtained in this paper have considerably benefited by the valuable remarks and discussions made by Dr. Y. Guldner, Dr. P. Voisin, and Dr. M. Voos of the Ecole Normale Supérieure Laboratory. I am glad to thank Dr. L. Esaki for his kind invitation at the IBM Laboratory and Dr. L. Esaki, Dr. L. L. Chang, and Dr. E. E. Mendez for helpful remarks.

\*Permanent address: Groupe de Physique des Solides de l'École Normale Supérieure, 24 rue Lhomond 75231, Paris Cedex 05, France.

- <sup>1</sup>L. Esaki, and R. Tsu, IBM J. Res. Dev. **14**, 61 (1970).
- <sup>2</sup>R. Dingle, in Festkörperprobleme XV (Advances in Solid Physics), edited by H. J. Queisser (Pergamon, Vieweg, 1975), p. 21.
- <sup>3</sup>L. Esaki and L. L. Chang, Thin Solid Films **36**, 285 (1976).
- <sup>4</sup>L. L. Chang, Proceedings of the XV International Conference on Semiconductors, Kyoto, 1980 [J. Phys. Soc. Jpn **62**, Suppl. A, 997 (1980)].
- <sup>5</sup>L. Esaki, in *Narrow Gap Semiconductors—Physics and Applications*, Vol. 133 of *Lecture Notes in Physics*, edited by W. Zawadzki (Springer, Berlin, 1980), p. 302.
- <sup>6</sup>G. A. Sai Halasz, L. Esaki, and W. A. Harrison, Phys. Rev. B **18**, 2812 (1978).
- <sup>7</sup>D. Mukherji and B. R. Nag, Phys. Rev. B **12**, 4338 (1975).
- <sup>8</sup>G. A. Sai Halasz, R. Tsu, and L. Esaki, Appl. Phys. Lett. **30**, 651 (1977).
- <sup>9</sup>G. Bastard, Phys. Rev. B **24**, 5693 (1981).
- <sup>10</sup>E. O. Kane, J. Phys. Chem. Solids **1**, 249 (1957).
- <sup>11</sup>S. White and L. Sham, Phys. Rev. Lett. **47**, 879 (1981).
- <sup>12</sup>D. J. Ben Daniel and C. B. Duke, Phys. Rev. **152**, 683 (1966); see also W. A. Harrison, Phys. Rev. **123**, 85 (1961).
- <sup>13</sup>N. W. Ashcroft and N. D. Mermin, *Solid State Physics* (Holt, Rinehart and Winston, New York, 1976), p. 146.
- <sup>14</sup>J. N. Schulman and T. C. McGill, Phys. Rev. B **23**, 4149 (1981).
- <sup>15</sup>See, for instance, Y. Guldner, C. Rigaux, A. Mycielski, and Y. Couder, Phys. Status Solidi B **81**, 615 (1977); **82**, 149 (1977).
- <sup>16</sup>C. R. Pidgeon, in *Handbook on Semiconductors*, edited by T. S. Moss (North-Holland, Amsterdam, 1980), Vol. 2; *Optical Properties of Solids*, edited by M. Balkanski (North-Holland, Amsterdam, 1980).
- <sup>17</sup>C. Lewiner, O. Betbeder, Betbeder-Matibet, and P. Nozières, J. Phys. Chem. Solids **34**, 765 (1973).
- <sup>18</sup>F. J. Ohkawa and Y. Uemura, J. Phys. Soc. Jpn. **37**, 1325 (1974).
- <sup>19</sup>J. M. Luttinger, Phys. Rev. **102**, 1030 (1956).
- <sup>20</sup>H. Bluysen, J. C. Maan, P. Wyder, L. L. Chang, and L. Esaki, Solid State Commun. **31**, 35 (1979).
- <sup>21</sup>Y. Guldner, J. P. Vieren, P. Voisin, M. Voos, L. L. Chang, and L. Esaki, Phys. Rev. Lett. **45**, 1719 (1980).
- <sup>22</sup>J. C. Maan, Y. Guldner, J. P. Vieren, P. Voisin, M. Voos, L. L. Chang, and L. Esaki, Solid State Commun. **32**, 683 (1981).
- <sup>23</sup>M. Combescot and C. Benoit à la Guillaume, Solid State Commun. **32**, 651 (1981).
- <sup>24</sup>P. Voisin, G. Bastard, C. E. T. Gonzalves da Silva, M. Voos, L. L. Chang, and L. Esaki, Solid State Commun. **32**, 79 (1981).
- <sup>25</sup>G. Bastard, Phys. Rev. B **24**, 4714 (1981).
- <sup>26</sup>L. Esaki, L. L. Chang, and E. E. Mendez, Jpn. J. Appl. Phys. **20**, L529 (1981).